

*Electronic Supplementary Information*

**Robust multiferroicity and magnetic modulation of the ferroelectric imprint field in heterostructures comprising epitaxial  $\text{Hf}_{0.5}\text{Zr}_{0.5}\text{O}_2$  and Co**

Tetiana Zakusylo,<sup>a</sup> Alberto Quintana,<sup>a</sup> Veniero Lenzi,<sup>b</sup> José P. B. Silva,<sup>c,d</sup> Luis Marques,<sup>c,d</sup> José Luís Ortolá Yano,<sup>a</sup> Jike Lyu,<sup>a</sup> Jordi Sort,<sup>e,f</sup> Florencio Sánchez,<sup>\*,a</sup> Ignasi Fina<sup>\*,a</sup>

<sup>a</sup>*Institut de Ciència de Materials de Barcelona (ICMAB-CSIC), Campus UAB, Bellaterra 08193, Barcelona, Spain. E-mail: [fsanchez@icmab.es](mailto:fsanchez@icmab.es), [ifina@icmab.es](mailto:ifina@icmab.es)*

<sup>b</sup>*Departament de Física, Universitat Autònoma de Barcelona, 08193 Bellaterra, Spain*

<sup>c</sup>*ICREA, Pg. Lluís Companys 23, 08010 Barcelona, Spain*

**Supporting Information 1**

In Figure S1, the leakage current vs voltage is shown. Leakage on samples with Co or Pt/Co electrodes is much larger than for the Pt case. This indicates that Co favors the presence of defects in the HZO layer.

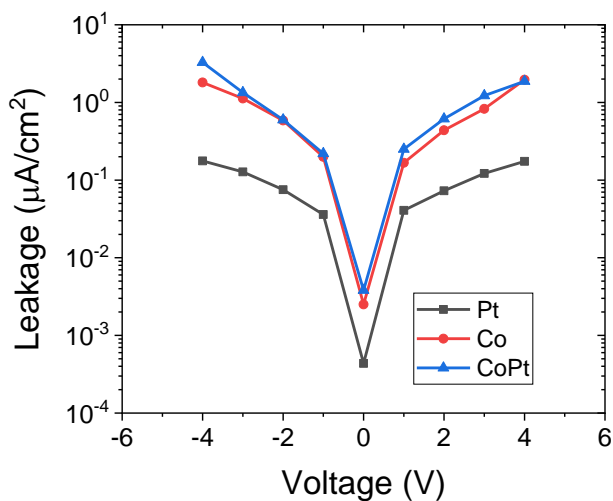


Figure S1. Leakage current for the Pt, Co and Pt/Co top electrodes.

## Supporting Information 2

Figure S2(a) shows microdiffraction XRD experiments, using 300  $\mu\text{m}$  spot width, underneath the three different groups of electrodes. Each group of electrodes covers approximately 1 mm, safely above the spot size. No difference on the position of the HZO peak can be detected. Figure S2(b) shows Hf 4f XPS spectra. Usually, traces of  $\text{Hf}^{3+}$  are taken as signature of oxygen vacancies deficiency.<sup>[16]</sup> However, the experimental resolution does not allow us to infer any difference among samples. Figure S2(c) shows the Co XPS spectra of HZO nominally equal samples with Pt(2nm), Pt(1 nm)/Co(1 nm) and Co(2 nm). Note that the thicknesses of both metals are not the same as those used in the characterization shown in the main text, to be able to detect the Hf and Co contributions. In this case, a larger intensity of the Co metallic peaks can be observed when measuring the Pt/Co sample. This indicates the greater amount of oxidized Co if Pt is not present.

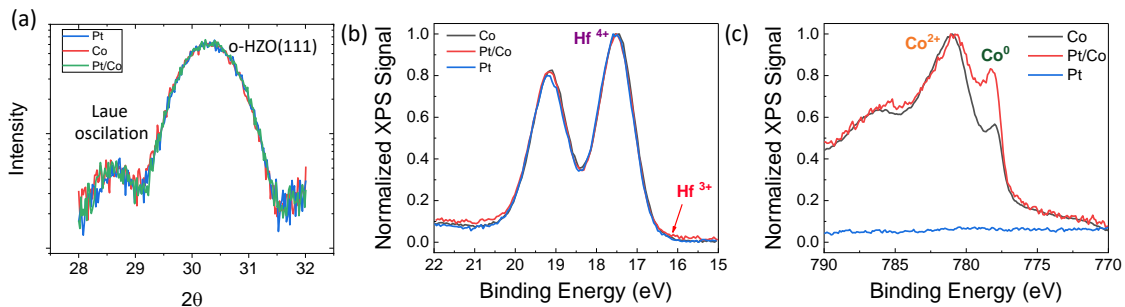


Figure S2. (a) XRD pattern performed by microdiffraction around orthorhombic (111) reflection of the Pt, Co and Pt/Co top electrodes. (b) Hf 4f, and (c) Co 2p XPS spectra for Pt, Co and Pt/Co top electrodes.

### Supporting Information 3

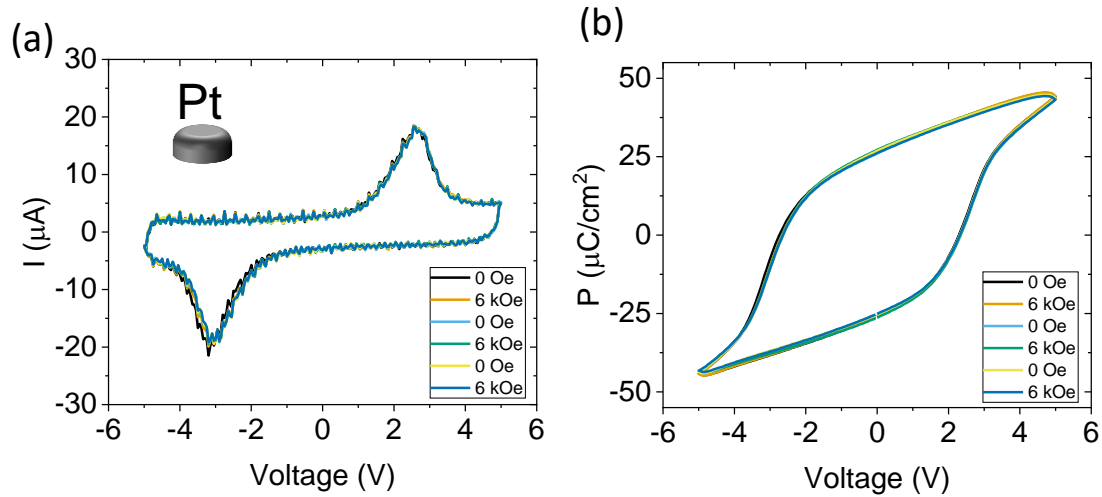


Figure S3. (a) I-V loops measured under 0 and 6 kOe, sequentially, measured in the HZO/Pt structure. (b) Corresponding P-V loops measured under 0 and 6 kOe.

### Supporting Information 4

Figure S4(a,b) show the dependence of capacitance on magnetic field with respect to its value at 0 Oe. In Figure S4(a), the same magnetic field range to that explored in the measurement of the P-V loops versus magnetic field (Figure 5) is explored. It can be observed that, despite the noise, the signal is constant. If the explored magnetic field is narrowed Figure S4(b), noise is reduced but similar absence of variation of capacitance on magnetic field is observed. By the same token, it can be concluded that extrinsic magnetoresistance effects<sup>[13]</sup> are absent in the measurement.

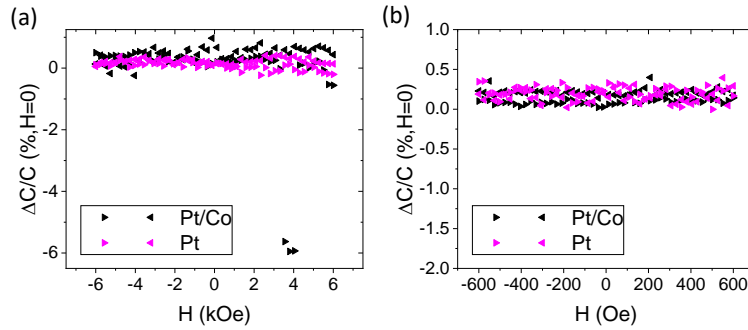


Figure S4. Capacitance as a function of magnetic field for the Pt and Pt/Co top electrodes.

### Supporting Information 5

Figure S5(a,b) shows I-V and P-V simulated loops, respectively, for different series resistance ( $R_s$ ) contributions to mimic series magnetoresistance effects (see inset). The loops have been simulated following the equations described in ref. [2] and the parameters have been selected to make the simulated P-V loops resemble those of the samples characterized in the main text. It can be observed that for  $1.05 \cdot R_s$ , comparable to Co magnetoresistance,<sup>[14]</sup> the simulated loop overlaps with the original. For  $1.50 \cdot R_s$ , the current peak positions [Figure S5a)] and coercive voltage [Figure S5(b)] are shifted to larger values, but in similar manner for both polarities, thus not resulting in an  $E_{imp}$  change, as experimentally observed. The I-V and P-V loops with 5% and 50% parallel resistance contributions have been also simulated [Figure S5(c,d)]. Similar effect to the series resistance contribution is observed. In the case of the I-V curves [Figure S5(c)], no significant change is inferred in the position of the current peaks, instead the current at large voltage increases for  $0.5 \cdot R_p$ . In the case of the P-V loops a symmetric increase of coercive voltage is seen for  $0.5 \cdot R_p$ , again not resulting in a  $E_{imp}$  change.

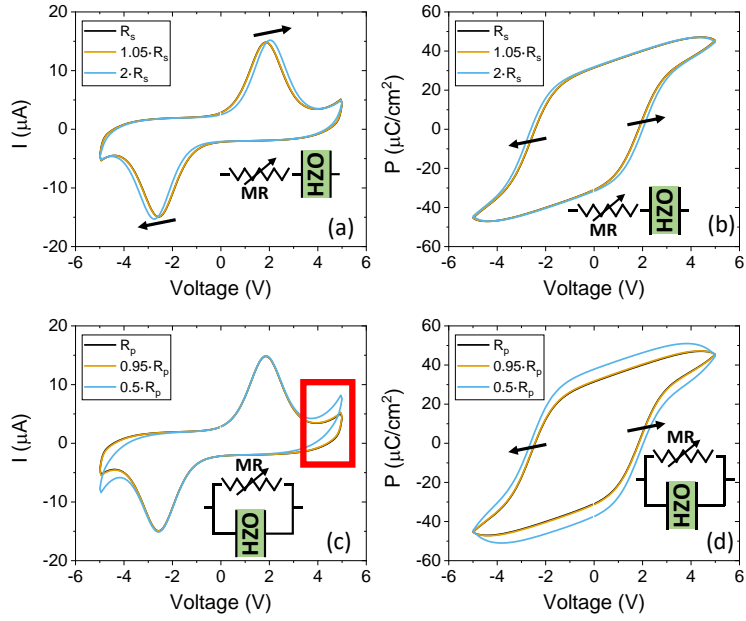


Figure S5. (a) I-V and (b) P-V loops for several  $R_s$  values as indicated. (c) I-V and (d) P-V loops for several  $R_p$  values as indicated.  $R_p$  and  $R_s$  variations mimic possible magnetoresistance contributions (MR).